SLAC-PUB-11276

LCLS-TN-05-31, May, 2005

Linac Coherent Light Source Longitudinal Feedback Model*

Juhao Wu†, P. Emma, L. Hendrickson, SLAC, Menlo Park, CA 94025, USA

Abstract

The Linac Coherent Light Source (LCLS) will be the world's first x-ray free-electron laser (FEL). To ensure the vitality of FEL lasing, it is critical to preserve the high quality of the electron beam during acceleration and compression. The peak current and final energy are very sensitive to system jitter. To minimize this sensitivity, a longitudinal feedback system on the bunch length and energy is required, together with other diagnostics and feedback systems (e.g., on transverse phase space). Here, we describe a simulation framework, which includes a realistic jitter model for the LCLS accelerator system, the RF acceleration, structure wakefield, and second order optics. Simulation results show that to meet the tight requirements set by the FEL, such a longitudinal feedback system is mandatory.

Introduction

Due to various sources of jitter in the LCLS accelerator system, it is envisioned that a longitudinal feedback system is mandatory [1]. In this paper, we describe such a facility.

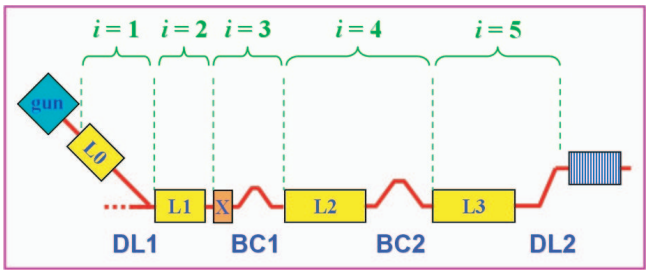

Figure 1: Schematics of the 5 stage LCLS linac-bend system.

In our model, we treat the LCLS accelerator system as a 5 stage linac-bend system as in Fig. 1. This model has been used to optimize the system for the operational parameters [1]. For the feedback, we assume that the controllables are the voltage dV/V and phase $d\varphi$ in the linac, while the observables are the peak current (bunch length) deviation dI/I, and centroid energy deviation dE/E of the bunch. So, we have 10 controllables and 10 observables to form a complete solvable linear system. The charge jitter and gun-timing jitter are left to the gun feedback system. Study on these two sources of additional jitter together with the jitter study in this paper will be reported elsewhere. In the real LCLS accelerator system the controllables are voltage of the L_0, L_1, and L_2; and the phase of L_1, L_2, and L_3. This is due to the fact that the bunch length does not change in DL1 or DL2, and also L1 and X-band ("X" in Fig. 1) are treated as a combined function cavity. Accordingly, there are 6 observables: energy at $DL1$, $BC1$, $BC2$, and $DL2$; and bunch length after $BC1$ and $BC2$. This is shown in Fig. 2. Conceptually, we regard it as a $4-$loop system, *i.e.*, $E_0 \leftrightarrow V_0$, $(E_1, I_1) \leftrightarrow (V_1, \phi_1)$, $(E_2, I_2) \leftrightarrow (V_2, \phi_2)$, and $E_3 \leftrightarrow \phi_3$.

Simulation Framework

Feedback algorithm The linear system is then $\mathcal{O} = \mathcal{M}\mathcal{C}$, with the observables column matrix $\mathcal{O} \equiv [(dE/E)_0, (dE/E)_1, (dI/I)_1, (dE/E)_2, (dI/I)_2, (dE/E)_3]^T$, the controllables column matrix $\mathcal{C} \equiv [(dV/V)_0, (dV/V)_1, (d\varphi)_1, (dV/V)_2, (d\varphi)_2, (d\varphi)_3]^T$, and $\mathcal{M}$ is the linear response matrix. The proportional feedback system is then implemented as

$$\mathcal{C}_{af} = \mathcal{C}_{bf} + \mathcal{G}\mathcal{M}^{-1}\mathcal{O}, \tag{1}$$

where $\mathcal{G}$ is the gain matrix, $\mathcal{C}_{bf}$ is the controllable states before the feedback, and $\mathcal{C}_{af}$ is the controllable states after the feedback is implemented. In defining $\mathcal{O}$ and $\mathcal{C}$, an "appropriate" set of subscripts according to Fig. 1 is adopted, *i.e.*, we follow the LINAC indices, *e.g.*, L0, but not the indices for the stages.

In the real situation, besides the proportional feedback, we need to also consider the derivative feedback and integral feedback, *i.e.*, the PID algorithm.

LINAC RF, Chicane, and Dog-leg In our model, we treat the LINAC RF as

$$E \rightarrow E + eV\cos(kz + \varphi), \tag{2}$$

where V is the peak voltage gain, k is the RF wavenumber, z is the bunch internal longitudinal coordinate, and φ is the centroid phase of the electron bunch. We also include the LINAC wakefield [2]

$$w(z) = \frac{Z_0 c}{\pi a^2} e^{-\sqrt{\frac{z}{s_0}}}, \tag{3}$$

where $s_0 \approx 1.32$ mm, and $a \approx 11.6$ mm for the SLAC S-band structure.

The chicane and dog-leg are modelled including second-order optics, *i.e.*,

$$z \rightarrow z + \delta\left(R_{56} + T_{566}\delta\right). \tag{4}$$

* Work supported in part by the DOE Contract DE-AC02-76SF00515. This work was performed in support of the LCLS project at SLAC.

† jhwu@SLAC.Stanford.EDU

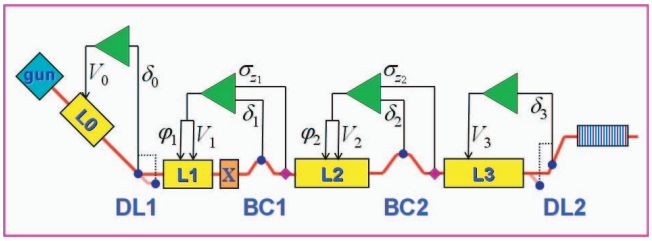

Figure 2: Schematics of the longitudinal feedback system.

Jitter model The voltage and phase variation are modelled as

$$\begin{pmatrix} \frac{dV}{V} \\ d\varphi \end{pmatrix} = \begin{pmatrix} A_1 \\ B_1 \end{pmatrix} \sin(2\pi f_1 t) + \begin{pmatrix} A_2 \\ B_2 \end{pmatrix} \sin(2\pi f_2 t) + \begin{pmatrix} A_3 \\ B_3 \end{pmatrix} t + \begin{pmatrix} A_4 \\ B_4 \end{pmatrix} \mathrm{randn}(1) + \begin{pmatrix} A_5 \\ B_5 \end{pmatrix} \sum_{j=1}^{N_{\rm step}} H(t - t_{{\rm step},j}) \quad \begin{bmatrix} \% \\ ^o \end{bmatrix}, \quad (5)$$

with $f_1 = 0.08$ Hz, $f_2 = 1.7$ Hz [1], "randn(1)" stands for a random number between 0 and 1 with normal distribution, and $t_{\rm step} = \tau \times {\rm rand}(N_{\rm step})$ with τ being the total rum time, and "rand($N_{\rm step}$)" stands for $N_{\rm step}$ random numbers between 0 and 1 with uniform distribution. The amplitudes are determined by the measurement, namely, $A_1 = B_1 = A_5 = B_5 = 1$, $A_2 = B_2 = A_4 = B_4 = 0.1$, and $A_3 = B_3 = 1/60$. Notice that, dV/V is in units of %, and $d\varphi$ in units of S-band degrees ^{o}.

Given this jitter, the "free" machine will operate as what is shown in the left panel of Fig. 3. Because a possible LCLS jitter budget is $|\Delta E/E| < 0.1\%$, and $|\Delta I/I| < 12\%$ at undulator entrance, obviously, without a feedback system we would not be able to meet the jitter budget.

Bode Plot

To study how such a feedback system works, let us look at the Bode plots. As usual, we introduce a quantity

$$\eta_E = 20 \log_{10} \left(\left| \frac{(\Delta E/E)_{on}}{(\Delta E/E)_{off}} \right| \right), \quad (6)$$

and vary the frequency of the system variations. We then vary the strength of the gain matrix $\mathcal{G}$ introduced in Eq. (1). As was discussed, we use the PID algorithm, hence, there is an optimization for the strength of these three different gain levels. Shown in Fig. 4 are three curves of η_E vs. frequency, for different PID gain. A similar Bode plot is found for $\Delta I/I$. According to our simulation, the derivative gain is not effective, while integral gain is effective. The Bode plots show attenuation of jitter for $f \leq 20$ Hz.

[1] The two frequencies f_1 and f_2 are based on SLAC linac measurements.

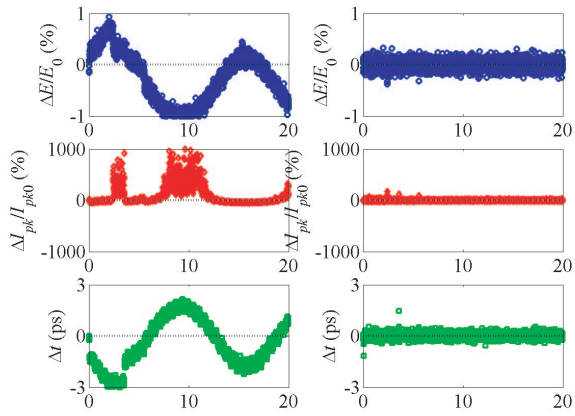

Figure 3: Energy deviation $\Delta E/E$, peak current deviation $\Delta I/I$, and centroid timing jitter Δt at undulator entrance. The left panel is shown for the case with no feedback, and the right panel with the feedback system on.

Results

Based on the Bode plot, we then use an I-gain of 0.5 alone. It is worth mentioning that, since we keep all the off-diagonal elements in the $\mathcal{M}$-matrix, we are indeed implementing a complete feedback algorithm, where local corrections are transmitted to downstream corrections. How this compares to multi-stage or single-stage cascade-feedback algorithm [3] is under study. The results are shown at the right panel in Fig. 3. The standard deviation values are: $\langle \Delta E/E \rangle_{std} = 0.09\%$, $\langle \Delta E/E \rangle_{std} = 10.5\%$, and $\langle \Delta t \rangle_{std} = 160$ fs. Hence, the allowable jitter budget can be accommodated. In our simulation, we implement CSR power as a relative bunch length monitor [4].

X-band RF Stability

In our algorithm, we do not implement direct feedback on the X-band cavity ("X" in Fig. 1). The strategy is to regard L_1 and L_x as a combined function cavity. So, let us now look at the possibility of adjusting the phase and voltage of L_1 to compensate the phase and voltage variations of L_x. According to Eq. (2), we know at the end of the X-band cavity, the electron energy is

$$E_2 = E_0 + eV_0 \cos(\varphi_0) + eV_1 \cos(\varphi_1) + eV_x \cos(\varphi_x), \quad (7)$$

with a linear chirp of

$$\mathcal{E} = -\frac{e}{E_2}[kV_0 \sin(\varphi_0) + kV_1 \sin(\varphi_1) + k_x V_x \sin(\varphi_x)]. \quad (8)$$

Now, according to Eqs. (7) and (8), to hold reference energy, (*i.e.*, E_2) and slope, (*i.e.*, $\mathcal{E}$) fixed, given X-band voltage change $\Delta V_x/V_x$, and phase change $\Delta\phi_x$, we have the following compensation relation of L1 voltage adjustment

	$\frac{\Delta V_x}{V_x}$ (%)			
	5	10	15	20
$\frac{\Delta V_1}{V_1}$ (%)	0.18	0.35	0.53	0.70
$\Delta\phi_1$ (^{o})	0.60	1.2	1.8	2.4
	$\Delta\phi_x$ (^{o})			
	5	10	15	20
$\frac{\Delta V_1}{V_1}$ (%)	-2.1	-4.3	-6.4	-8.5
$\Delta\phi_1$ (^{o})	2.1	4.2	6.3	8.4

Table 1: Adjustment of L_1 phase and voltage to compensate L_x phase and voltage changes.

$\Delta V_1/V_1$, and phase adjustment $\Delta\phi_1$

$$\begin{pmatrix} \frac{\Delta V_1}{V_1} \\ \Delta\phi_1 \end{pmatrix} = \frac{V_x}{V_1} \begin{pmatrix} -\cos\phi_1\cos\phi_x - \frac{\lambda}{\lambda_x}\sin\phi_1\sin\phi_x \\ \sin\phi_1\cos\phi_x - \frac{\lambda}{\lambda_x}\cos\phi_1\sin\phi_x \\ \cos\phi_1\sin\phi_x - \frac{\lambda}{\lambda_x}\sin\phi_1\cos\phi_x \\ -\sin\phi_1\sin\phi_x - \frac{\lambda}{\lambda_x}\cos\phi_1\cos\phi_x \end{pmatrix} \begin{pmatrix} \frac{\Delta V_x}{V_x} \\ \Delta\phi_x \end{pmatrix}. \quad (9)$$

In our design, we have $\lambda \approx 10.5$ cm, $\lambda_x = \lambda/4$, $\phi_1 = -25^o$, $\phi_x = -160^o$, $V_1 = 147.39$ MeV, and $V_x = 19.0$ MeV. According to Eq. (9), we have the following L_1 response given L_x changes in Table 1.

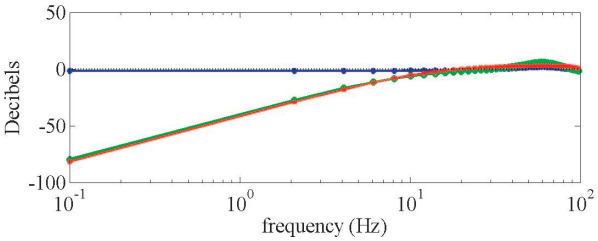

Figure 4: Bode plot for $\Delta E/E$. The vertical axis is for η_E defined in Eq. (6). The blue curve is for P-gain of 0.2; the green for P-gain 0.2 and I-gain 0.5; and the red I-gain 0.5.

On the other hand, let us look at the simulated feedback response. We introduce the same changes in the X-band cavity, and the corresponding response of the L_1 RF is plotted. In Figs. 5 and 6, we show the L_1 voltage and phase adjustment for an L_x voltage change. Similarly, we also study the L_1 adjustment for an L_x phase change (not shown). We find the feedback algorithm can correct the L_x RF changes by adjusting L_1 RF accordingly, and the results are quite close to the linear estimate given in Table 1, especially for small X-band errors. It is worth pointing out that, it would be sufficient, if L1 can correct up to $\pm 2.5\%$ voltage error, and $\pm 5^o$ phase error of the X-band cavity. The simulation shows that the feedback system does have such an ability.

Discussion

According to the study in this paper, a longitudinal feedback system is mandatory to ensure LCLS lasing stability. With such a feedback system, the prescribed system jitter budget can be met. In real implementation, one has to consider the imperfect calibration, and also the resolution of bunch length monitor, BPM, etc.. All these have been tested in the simulation to certain level, however, further study is needed to fully optimize the feedback system. As we mentioned above, the gun jitter is used as an input to this $6-$D feedback system. However, the energy feedback in chicanes causes $1-$to-1 gun-timing to final timing jitter [5], hence, further study on the two feedback systes, *i.e.*, the gun feedback system, and the linac feedback system described in this paper, is needed and underway.

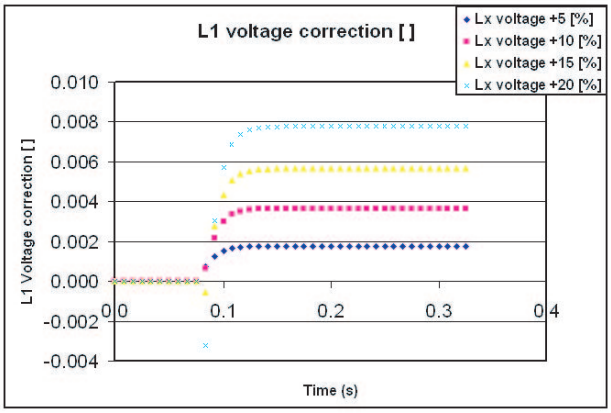

Figure 5: Adjustment of L_1 voltage for L_x voltage change.

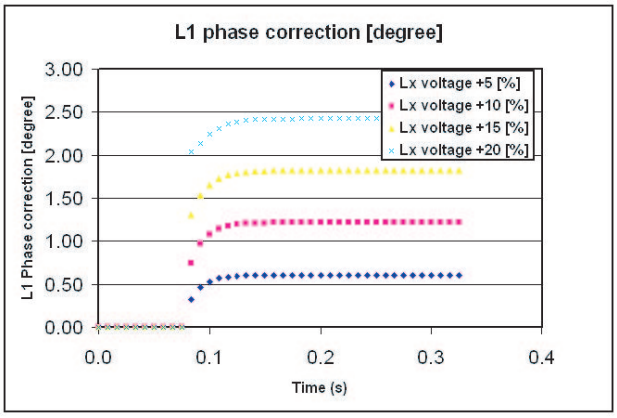

Figure 6: Adjustment of L_1 phase for L_x voltage change.

The authors would like to thank E. Bong, D. Dowell, and P. Krejcik for many useful discussions.

REFERENCES

[1] P. Emma, in SLAC Report No. SLAC-R-593 (2002).

[2] K.L.F. Bane, in SLAC Report No. SLAC-R-593 (2002).

[3] T. Himel, *et al.*, PAC 93, 2106 (1993).

[4] J. Wu, P. Emma, and Z. Huang, these PAC'05 proceedings.

[5] P. Emma, "Timing jitter with energy feedback", talk given at XFEL workshop, SLAC, July 26 - 30, 2004.